Caging and Geminate Recombination following Photolysis of Triiodide in Solution

Erez Gershgoren, Uri Banin, and Sanford Ruhman*

Department of Physical Chemistry, and the Farkas Center for Light Induced Processes, The Hebrew University, Jerusalem 91904, Israel

Received: July 2, 1997; In Final Form: September 24, 1997[⊗]

A survey of caging and geminate recombination dynamics following the UV photolysis of I_3^- in a series of polar solvents is presented. Transient absorption in both the near-IR and UV was measured out to delays of 0.4 ns, probing evolution of the nascent product and recombined reactants, respectively. The fate of photolysis fragments is suggested to be determined shortly after the act of bond fission. Kinetic analysis shows caged fragments either recombine directly and vibrationally relax within a few picoseconds or produce long-lived complexes of unknown structure that decay exponentially in ∼40 ps, and both routes lead to ground-state I_3^-. The persistent complex exhibits a near-IR absorption spectrum that is broadened and red-shifted relative to free I_2^-. A very shallow and slow residual component of recombination may be associated with encounters of geminate pairs that initially escape the solvent cage. The choice of solvent strongly effects the probability and dynamics of caging, but not the decay rate of complex caged pairs. This is not altered by varying the temperature of an isobutyl alcohol solution from 5 to 45 °C. The results are discussed in an effort to illuminate the role played by the solvent in triiodide recombination in solution.

I. Introduction

Geminate recombination of photolysis fragments in condensed phases is the subject of active theoretical and experimental study. The driving force for this scrutiny stems from this processes fundamental nature, the accumulating efforts already invested in its elucidation, and the importance of solvent caging as a major limiting factor of practical photochemical transformation. Early efforts at representing this process are based upon diffusion-limited descriptions[1−3] and despite their tenure have not lost their intuitive appeal.[4,5] More recent real time studies of small molecule photolysis show that mutual diffusion of separated fragments is only a secondary route to solvent-induced geminate recombination.

In molecular liquids iodine predissociation plays an active role in the dephasing of impulsively excited coherent B state wave packets,[6−8] and subsequent recombination onto various bound potential surfaces takes place within less than 2 ps.[9] Dynamical models used to explain these results show that most geminate recombination takes place within the confines of the initial solvent cage and not by cage escape followed by diffusive encounters in the solvent. The nonadiabatic processes that allow these transitions have been further scrutinized through spectroscopic probing of iodine photophysics in rare gas solids.[10−12] Similar experiments in high-density rare gas fluids again highlight the prominent and distinct part played by direct cage reformation of the reactants.[13]

For I_2^- in polar liquids, despite marked differences in the range and intensity of solute−solvent forces, the act of recombination and loss of excess vibrational energy following photodissociation are also extremely rapid. Experiments both in gas-phase clusters and in solution show that curve crossing to the ground state and most of the vibrational relaxation are achieved by the recombining molecules very rapidly, and in liquid solutions this takes place in a fraction of a picosecond.[14−19] The residual separated population in solutions persists for the duration of the experiments, with no convincing indication of a diffusive recombination component. Thus in both systems, despite their differences, cage-induced repopulation of the ground state is not separated in time scale from the bond fission itself, rendering both a single unified dynamic process.

The photodissociation of triiodide and more recently I_2Br^- has been studied by impulsive femtosecond laser photolysis in a variety of polar molecular solvents[20−24]

$$I_3^- + h\nu \rightarrow I_2^{\bullet -} + I^{\bullet}$$

All studies conducted in our lab involved photoexcitation of triiodide ions at 308 nm, just to the red of the more energetic and intense near-UV band centered at ∼295 nm. The strong near-IR spectrum of the diiodide has been used to follow the emerging fragment ions, while probing at the excitation frequency mapped out dynamical changes in the I_3^- remaining in the ground state.

Reports have focused on the dynamics of bond fission and the generation of coherently vibrating diiodide molecular fragments. Spectral modulations in the near-IR transient transmission signals indicate that the compact coherence induced by the impulsive photoexcitation transcends bond fission and evolves continuously into compact coherent motion in the product. This finding was supported by quantum and classical MD simulations that demonstrate how preservation of phase coherent nuclear motions throughout dissociation might take place, despite the presence of solvent surrounding the reacting molecule.[25−27] Simulations were conducted employing a LEPS form reactive potential that was not the result of detailed calculation of electronic structure, and in particular, no routes

[⊗] Abstract published in *Advance ACS Abstracts,* December 1, 1997.

S1089-5639(97)02138-5 CCC: $15.00
Published on Web 01/01/1998

for nonadiabatic relaxation back to the ground state were considered. Recently, the role of symmetry breaking in preservation of coherence in photofragment vibrational motion has also been addressed, by comparing the triiodide reaction dynamics with those of asymmetric I_2Br^-.[24]

Nonetheless, experimental probing at longer delays did show obvious signs of solvent-dependent geminate recombination following trihalide photolysis.[21] Nonexponential multiphased regeneration of reactant absorption along with a concurrent disappearance of product OD was the key observation. The absorption kinetics were followed for less than 100 ps.

While delayed recombination mechanisms were not determined, possible recombination routes were considered.[21,22,25] Since I_3^- is routinely synthesized by reacting I^- with I_2, it is plausible that geometrical or energetic restrictions might limit the rate of recombination from the I_2^-/I channel. Furthermore, the excess photon energy suffices for producing either of the fragments in low-lying excited electronic states.[18] Therefore, electronic relaxation or electron transfer might be required to open the way to recombination, and such pairs would constitute separate kinetic routes to the ground state.

More recently, an ultrafast laser study of triiodide photolysis and geminate recombination dynamics was conducted with superior time resolution, exciting into the lower of the near-UV bands with ∼395 nm excitation pulses.[28] At this wavelength both relaxed I_2^- and I_3^- absorb considerably, making probing at that frequency of limited utility in covering the process of recombination. I_3^- kinetics were reconstructed directly from the IR data. Despite the close resemblance to recombination results following excitation with 308 nm pulses, it has been interpreted in a very different light, in terms of a diffusion-limited geminate recombination model, producing kinetics with stretched exponential appearance. Absorption kinetics were covered only for a limited delay range.

The present study is intended to broaden our understanding of the mechanisms underlying triiodide caging and recombination following 308 nm photolysis, by recording pump−probe data with high time resolution, extending out to long probe delays, including measurement of signal dependence upon variation of solvent and its temperature. Given a conceptual framework whereby the crucial electronic and vibrational relaxations redirecting excited density back to the bound states of the reactant take place hand in hand with the process of bond fission, it is impossible to comprehend one without the other. Therefore, a full understanding of the generation of phase coherent motion in fragments due to impulsive photodissociation of the parent ion requires both processes to be studied as a whole and incorporated into a refined theoretical model of this reaction.

Results reported in this paper demonstrate that the multiple components of I_3^- recombination following 308 nm photolysis are most likely due to distinct pathways, none of which is obviously controlled or limited in rate by mutual diffusion of the fragments. As in the case of the similar diiodide system, data are interpreted to indicate that most recombining I_3^- never escapes the solvent cage, and the division into recombinant and dissociating populations, which takes place at the initial stages of dissociation, is strongly dependent upon the nature of the solvent.

The paper is organized as follows: Section II provides a brief description of the experimental system and methods. Section III is dedicated to a detailed account of the experimental results. In section IV these results are discussed, and a simple kinetic model is proposed for their interpretation. Conclusions of the present study and a summary of remaining undetermined issues are presented in section V.

II. Experimental Section

The laser system and general methods of sample preparation have been discussed in detail elsewhere.[21] The homemade synchronously pumped and amplified dye laser system provides a kilohertz train of ∼65 fs pulses, centered at 615 nm, containing ∼40 μJ of energy. These were used to generate pump pulses by frequency doubling in $^1/_2$ mm of KDP, and probe pulses were derived either in an identical fashion for UV/UV experiments or by white light generation in a sapphire flat followed by interference filtering for visible and near-IR probes. Transmission was detected by amplified photodiodes (EG&G UV-4000) and measured with a lock-in amplifier (SRS 530). All solvents used were either spectroscopic or HPLC quality, and triiodide was produced using resublimed iodine crystals and high-purity KI.

The long scans of probe delay required extra care that results are free of sample concentration, laser power, and pump−probe overlap walk-off dependence. Each scan was first run at a pump power 2−3 times higher than that ultimately used when collecting data, and linearity of the results with power was demonstrated. Trial runs were recorded using solutions nearly 10 times more concentrated than those actually employed to collect data (in a thinner circulating sample cell), and the results were virtually superposable with those obtained at lower concentrations. Data presented here were collected from solutions of ∼0.25 mM concentration, with a mild excess of iodide, which were circulated through a 2 mm cell using a peristaltic pumping station. The UV−vis absorption spectrum of the solutions was monitored both prior to the experiments and after, with no observable deterioration of the sample in any of the solutions employed. Flow rates ensured replenishment of fresh sample for each pulse.

Fine alignment of the beams ensured that their transmission through a 100 μm pinhole at the sample position was independent of the pump−probe delay throughout the range studied. Without this precaution substantial artifactual decays in the data resulted for delays beyond a few tens of picoseconds. The experiments aimed at testing the temperature dependence of recombination kinetics in isobutyl alcohol solutions were conducted by submerging the sealed sample reservoir in a controlled temperature bath. The temperatures at the cell were determined by a thermometer and found to differ by no more than 2−3 deg from that of the bath.

III. Results

Data obtained for ethanol solutions, which were most thoroughly studied, will be presented first. A UV transient transmission scan spanning delays from 0 to 400 ps is depicted in Figure 1. To facilitate the presentation of rapid transmission changes taking place at early delay times, an inset of the first 8 ps of delay is presented on an expanded time scale. The positive going signal here relates negative changes in OD, indicating that photolysis induces a bleach in the triiodide absorption. The rapid component of decay, which is complete in less than 6 ps, is superimposed with periodical oscillations that have been reported in detail and stem from impulsive resonant Raman excitation of the symmetric stretch of the triiodide ion.[28−30] This portion of the data is fit to an exponential decay summed with a damped harmonic oscillation.

Following this initial rapid stage of UV bleach recovery, a continued but slower decrease in transmittance commences

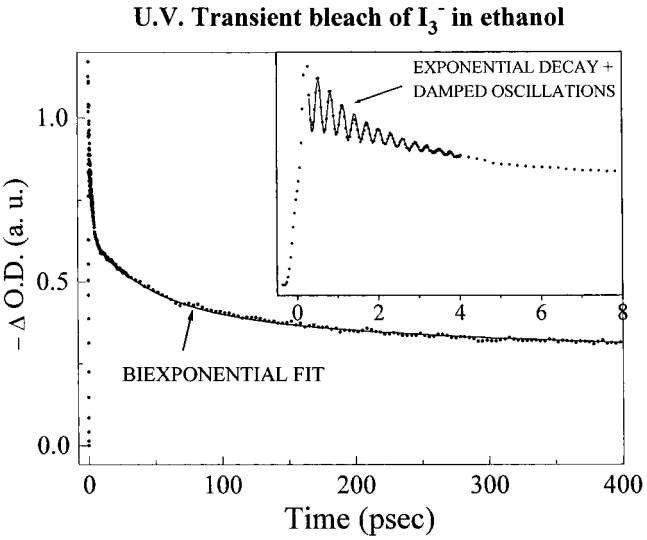

Figure 1. Transient transmission scans of triiodide in ethanol solution with both UV pump and probe pulses. The inset depicts the first 8 ps of probe delays, exhibiting a rapid decay of the initial bleach superimposed by impulsive Raman-induced spectral modulations. See text for details.

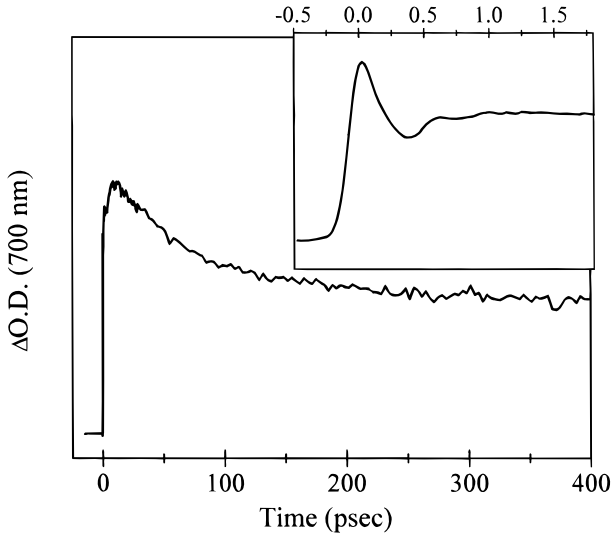

Figure 2. Transient absorption scan at 700 nm following 308 nm photolysis of triiodide in ethanol solution. The inset shows the first 2 ps of probe delay within which spectral modulations due to vibrational coherence in photoproducts is observed.

which takes place in two stages, the first of which is completed in ~100 ps gives way to a very gradual and shallow decay component. The later portions of transmission decay beyond 11 ps are presented along with a fit to a biexponential functional form

$$T(t) = A + B\exp(-t/\tau_1) + C\exp(-t/\tau_2) \qquad (1)$$

The constants used for this fitting will be discussed in detail later.

Along with UV transmission measurements, transient OD scans throughout the near-IR were also recorded. Transient absorption at 700 nm extending up to 400 ps, following UV excitation at $t = 0$, is presented in Figure 2. This wavelength is near the center of the relaxed diiodide band. The inset depicts the first 2 ps of absorption evolution, exhibiting an initial phase of absorbance attributed to the dissociative excited state, which decays as the bond fission occurs (collected in a 0.2 mm cell

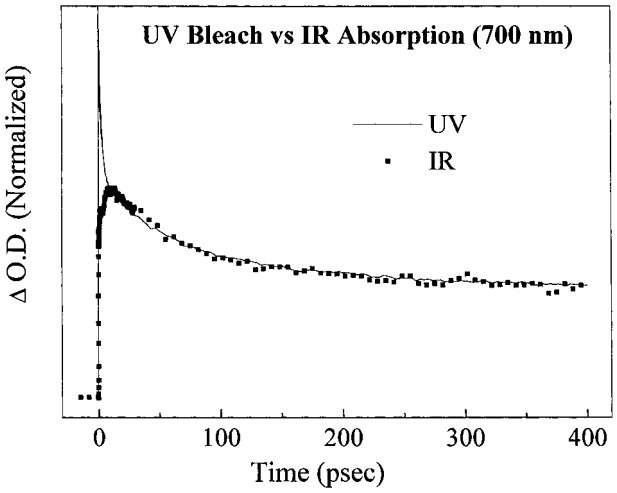

Figure 3. Comparison of bleach kinetics at 308 nm with transient absorption at 700 nm following triiodide photolysis in ethanol. Both signals have virtually the same decay after the initial 10 ps of pump−probe delay.

for obtaining high time resolution). The spectral modulations that are observed following this stage were the focus of previous studies and attributed to coherent vibrations of fragment ions. They are superimposed upon an increase of signal associated with vibrational relaxation of hot fragment ions and partly to absorption of cooling recombinant triiodide. At 700 nm these modulations are particularly weak since this wavelength is near the center of the product band and are more pronounced both to the red and to the blue.

After ~10 ps, a gradual nonexponential decay in absorbance commences, which is similar in appearance with that of the later stages of bleach recovery in the UV. This similarity is demonstrated in Figure 3, which depicts UV bleach kinetics together with the decay of 700 nm absorption in adjusted units that achieve normalization of both signals at a 400 ps delay. The signals effectively match each other continuously after an initial delay of ~10 ps. A similar scan was presented in the initial report of the ultrafast study of this reaction, as a consistent measure of the recombination dynamics of dissociated I_3^-. The rationale behind this assertion was that, following an initial stage of solvation and vibrational relaxation, absorption in the near-IR is due solely to I_2^- radicals, while that in the near-UV is indigenous to the triiodide. Thus, recombination would contribute linearly to the disappearance of the first and reappearance of the later.

To investigate this further, a series of transient absorption scans at various near-IR probing frequencies were collected and are depicted in Figure 4. In the first panel the absorption scans are plotted on a vertical scale that shows the relative intensities of absorption at the various wavelengths. The second panel depicts the same data after arbitrary vertical scaling in order to normalize all scans to the same intensity at long delay times. From 130 to 400 ps the scans overlap remarkably well. But at earlier times that are yet much later than the duration of vibrational relaxation, there is no agreement between the various curves. The mismatch is systematic, showing larger relative intensities for the more red-shifted spectral components. This trend was also obtained for a less complete series of IR data collected in isobutyl alcohol solution.

In view of the roughly complementary nature of the UV bleach and IR absorption, and in accordance with a kinetic model to be outlined in the following section, the IR data in ethanol for delays beyond 11 ps were also fit using eq 1 with

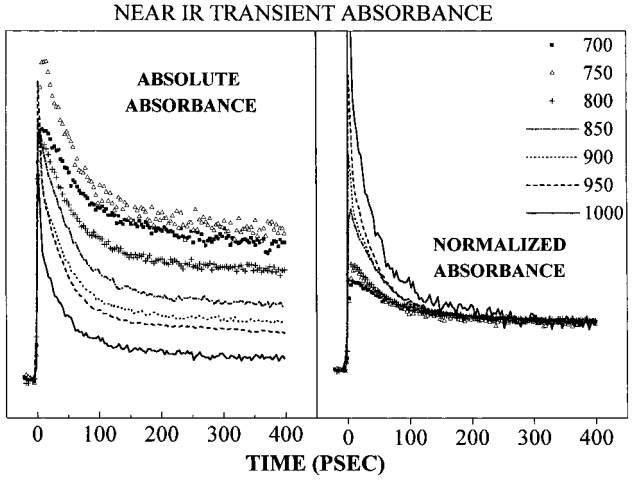

Figure 4. Transient absorption at various near-IR wavelengths plotted on two scales. The first frame depicts the scans on a correct relative scale, while the second has normalized all scans to the same intensity at 400 ps.

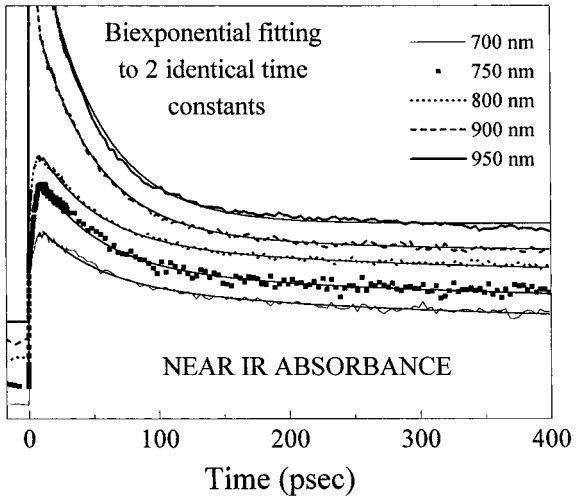

Figure 5. Demonstration of the quality of fit rendered by an offset biexponential described in eq 1 to the near-IR data at various probing wavelengths. All fits employ the same decay constants with varying relative amplitudes.

the same decay constants that optimally fit the UV/UV data. This portion of the data, on offset and expanded scales, is plotted along with the fit in Figure 5. As demonstrated, a single pair of constants provides a good rendition of the data at the various frequencies.

In an effort to further identify the mechanisms for various stages of trihalide recombination after dissociation, UV transmission scans were conducted for triiodide solutions in ethanol, water, acetonitrile, and isobutyl alcohol, also to be augmented by previous data in methanol and 1-propanol solutions. Results are summarized in Figures 6 and 7 for the first four solvents mentioned. Figure 6 presents the earlier portion of the signals along with a fit of the modulation to a damped harmonic oscillation riding atop a rapid exponential decay. In the case of isobutyl alcohol a deviation from exponentiality required fitting the underlying decay to a third-order polynomial function. The best fitting parameters are summarized in Table 1.

Figure 7 shows similar scans which include delays from 0 to 400 ps for the first four solvents. The vertical scales have been normalized to rise from 0 to 1 between the signal at negative times to the peak of the underlying signal minus the oscillating component which is associated with the impulsive Raman

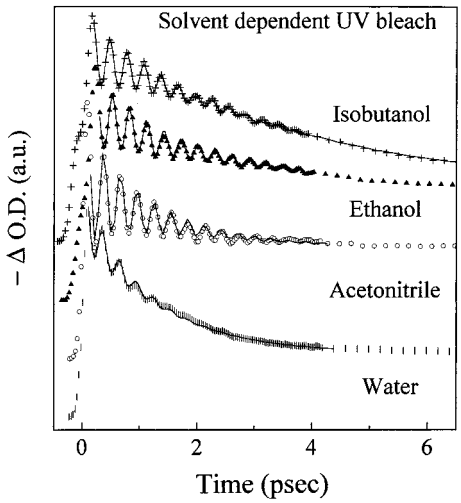

Figure 6. Evolution of the fast component of UV bleach in four solvents, along with fits that reproduce the decay of the bleach as well as the periodic modulations. Details of the constants used are summarized in Table 1. The bleaches are normalized to the same peak intensity and offset to facilitate their demonstration.

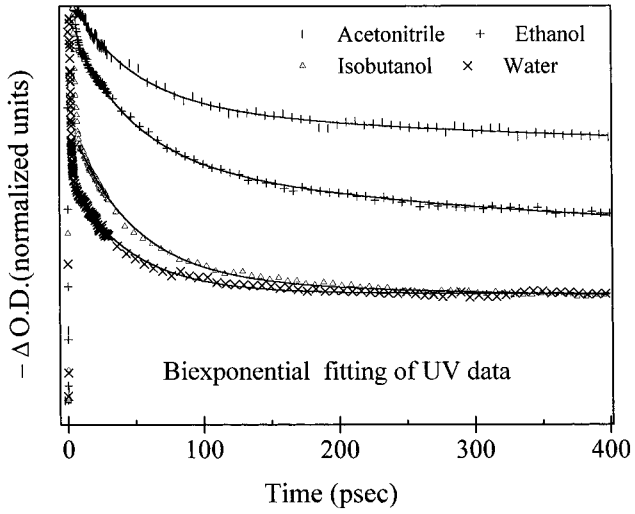

Figure 7. Solvent dependence of the later stages of UV bleach in four solvents, along with the fit to eq 1 using the same two decay constants that best fit near-IR decays in ethanol solutions.

TABLE 1: Fitting Constants for Fast Component

solvent	τ_{phase} (ps)	ω (cm^{-1})	τ_{decay} (ps)
water	0.53	112.5	1.3
CH_3CN	0.89	114	1.5
ethanol	1.2	112	2.6
isobutyl alcohol[a]	1.0	112	~4

[a] Nonexponential decay.

mechanism. A number of trends are observable. The initial very prompt decay of the bleach is most prominent in water and isobutyl alcohol and weaker in ethanol and acetonitrile. In all these solutions the decay of the bleach is again well reproduced by a biexponential decay which does not return to zero, where the smallest absorption recovery is observed for acetonitrile and the highest in water and isobutyl alcohol.

The same two decay constants employed for fitting the UV bleach decay in Figure 1 are employed for delays larger than 11 ps, albeit with varying amplitudes, to provide satisfactory fits to the UV data in Figure 7. The amplitudes of the various components required for fitting are summarized in Table 2, along with the amplitude of the prompt decays required to sum the

TABLE 2: Amplitudes of F/M/S UV Decay Components

solvent	"fast"	*B*	*C*	*A*
water	0.62	0.2	0.0	0.18
CH_3CN	0.29	0.19	0.084	0.44
ethanol	0.34	0.23	0.14	0.27
isobutyl alcohol	0.42	0.27	0.04	0.18
methanol[a]	0.15			

[a] From earlier study (U. Banin).

signal to 1, designated as $1 - (A + B + C) \equiv$ "fast". The table also gives a partial analysis for data not plotted here, obtained in other solvents.

Finally, to test the dynamics of geminate recombination in a single solvent at various temperatures, the UV transmission was recorded for a solution of triiodide in isobutyl alcohol at temperatures between 5 and 50 °C. Since the results were exactly superposable with the data in Figure 7 for this solvent throughout this temperature range, data are not presented here.

IV. Discussion

(a) Criteria for Kinetics of Recombination. The goal of this study is to follow the process of geminate recombination following the UV photolysis of I_3^- in polar solvents. Accordingly, data were collected for delays that temporally span the gap between femtosecond studies and earlier conventional flash photolysis experiments on this system. Analysis of these data must include a review of the assumptions used previously to interpret our results, i.e., (1) that near-IR absorption recorded in the data is due solely to free diiodide fragments at all time delays and (2) that the transient UV absorption at 308 nm monitors the concentration of relaxed I_3^- selectively and quantitatively.

In both the red and UV, rapid changes of absorption have all but leveled off at the far limit of our observation window, indicating that ~0.5 ns is a sufficient delay for covering all the stages of geminate reformation of the reactants. Accordingly, the asymptotic transient IR spectrum must match that of I_2^- from the literature,[31−33] which is the sole primary near-IR-absorbing product following nanosecond flash photolysis of triiodide solutions. For comparison, the data in Figure 4 are employed to reconstruct the asymptotic absorption spectrum at a delay of 400 ps and displayed along with one from the literature in Figure 8, showing that the spectra agree well within error (determined by repeatability of pump/probe overlapping at different probing frequencies). Thus, the assumption that at the longest delays covered diiodide remains the sole stable IR-absorbing photofragment to escape geminate recombination is consistent with the data. Furthermore, in view of the second panel in Figure 4, the transient absorption matches that of free I_2^- already at a delay of ~150 ps, since all probing frequencies produce identical decay kinetics from that delay onward.

Now one can apply the conclusion above to test assumption 2, concerning the UV absorption as a quantitative measure of the I_3^- concentration. If the UV absorption at 308 nm is due solely to the strongly absorbing I_3^- throughout the scans,[34] the ultimate escape probability of nascent I_2^-/I fragments can be obtained directly as the ratio of the asymptotic UV OD bleach (proportional to the concentration of nonrecombined triiodide at the end of the geminate reformation) to its initial value. This can be further tested by comparing escape probabilities so obtained with ones measured by nanosecond flash photolysis.

Reviewing the data in Figure 7, and the constants in Table 2, lead to an escape probability of nearly 50% in acetonitrile, one of about 33% in ethanol solution, and even smaller yields

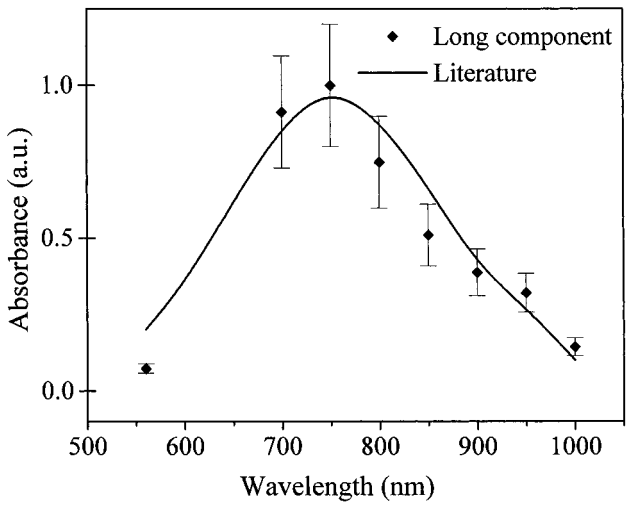

Figure 8. Coarse-grained transient spectrum in the IR 400 ps after 308 nm excitation of triiodide in ethanol, along with that of diiodide from the literature.

in water and in isobutyl alcohol. In a related study, flash photolysis experiments using 1 ns N_2 laser pulses recorded a transient absorption spectrum following the photoexcitation in both ethanol and acetonitrile.[35] From absolute measurement of the excitation pulse flux and the instantaneous ΔOD at $\lambda_{max}(I_2^-)$, the escape probability was measured to be between 40 and 50% in acetonitrile and 30 and 40% in ethanol. In view of the large margin of error in the nanosecond experiments, the small change in excitation photon energies used for the two experiments is ignored. These results agree remarkably well with the values derived from the UV transmission data described above. In light of this, the assumption that the 308 nm transients serve to directly monitor relaxed triiodide concentrations will be adopted. Assumption 1 has not yet been verified for all delays, however.

(b) Kinetic Schemes for Recombination. We turn now to unraveling the dynamics at intermediate times. The appearance of the UV data suggests that distinct temporal phases characterize the regeneration of the reactants, starting with an ultrashort initial phase of a few picoseconds, which is attributed to a direct recombination mechanism, the duration of which is strongly solvent dependent, as demonstrated by the fitting constants in Table 1. Since the duration of this phase must include both the time required for repopulation of the ground state and the duration of vibrational relaxation, it is not surprising to find that it is shortest in water and most prolonged in isobutyl alcohol. Water should be the most efficient solvent in extracting excess vibrational energy from highly excited recombinant triiodide ions, with the heavier alcohols being least effective in this respect.

As can be observed from Table 1, a similar trend is also found in rates of dephasing of the vibronic coherences. It is important to stress that the overall replenishment of the reactant absorption must deal with recombination and vibrational relaxation from very high-lying vibrational levels of triiodide down to the thermally occupied region of phase space. In contrast, the spectral modulations reflect coherences built up from low-lying vibronic states of ions that ultimately remain on the ground electronic surface, as demonstrated in earlier simulations.[21,30] As for the nonexponential behavior of bleach decay in the case of the heavy alcohol, since we are not dealing with a two-level system but rather replenishment from a whole manifold of states, this would be expected to be the rule and not the exception. In

the case of the more rapidly relaxing solvents it is remarkable that a single exponential does such a good job of fitting the kinetics.

The most complex phase of recombination dynamics follows this initial prompt component, leading up to the asymptotic stage at the latest observation times. The nonexponential reformation kinetics following the initial "direct" phase of recombination might be characterized by the simple scheme

SCHEME 1

$$I_3^- + h\nu \leftrightarrow I_2^{\bullet -} + I^\bullet$$

Here the geminate recombination which extends beyond the direct reformation requires diffusive encounters of separated fragment pairs as described by Kuhne and Vohringer[28] and is expected to produce nonexponential kinetics. According to this scheme, absorbance changes both in the UV and throughout the near-IR would exhibit identical kinetics (including not only decay constants but also identical relative amplitudes) since it entails disappearance of one absorbing species solely responsible for near-IR absorption, diiodide, and reappearance of another exclusively absorbing in the 300−350 nm region, relaxed triiodide (with a negligible delay effect caused by the vibrational relaxation of the most recently recombined reactants). This requirement is obviously violated in the scans depicted in Figure 4, where the IR absorption kinetics demonstrate a strong wavelength dependence well beyond the first 20 ps of delay.

Furthermore, had a simple diffusive geminate recombination mechanism been responsible for reconstitution of triiodide, a significant change in the rate of this process would be expected upon changing the viscosity of the solvent, either by variation of the solvent altogether or by altering the solutions temperature as described above. This is not observed and must indicate that an alternative mechanism underlies the recorded kinetics.

A biexponential functional form was initially utilized for fitting data in both the IR and UV without reference to any specific kinetic model. Furthermore, in view of the slow evolution and incomplete coverage of the shallow decay, the second exponent ($\tau_2 = 350$ ps) is poorly determined and effectively provides a very gradual tapering of the data at long delays. While in practice kinetics produced by diffusion-controlled models can resemble a biexponent over limited temporal ranges, the observation that spectral evolution in the near-IR is limited to the intermediate phase of reformation is telltale, suggesting that in fact the mechanisms leading to the strong recombination in the 10−100 ps regime is separate and distinct.

The simplest kinetic scheme capable of reproducing the observed transient transmission kinetics might be constructed as follows:

SCHEME 2

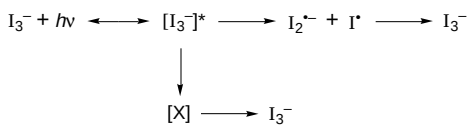

According to Scheme 2, aside from the directly caged and recombined reactants, two independent reactive channels exist, one leading to separated I_2^- and I radicals and the other to produce an as yet unidentified intermediate that ultimately reforms the triiodide reactant on a time scale of a few tens of picoseconds. Since all of the recombination processes that supersede the direct portion are much slower than vibrational relaxation of molecular ions in polar solvents, the near-IR spectrum at delays beyond 10 ps will be a superposition of that of X and that of I_2^-, weighted by their instantaneous concentrations. Furthermore, if the kinetics of each of these channels is reasonably represented as exponential, the transient absorption will follow a biexponential decay characterized by the same two decay constants, but with changes in the relative amplitudes according to the extinction coefficients of X and diiodide at the specific wavelength. Finally, since both components of decay in IR absorption are due to recombination to produce I_3^-, the same constants will also adequately characterize the kinetics of replenishment in absorbance of the reactant.

The above simplistic scheme explains why, despite the fact that individual scans might be best fit to somewhat varied constants, we sought out a single combination that produced very good fits to all the collected data in both the UV and near-IR for ethanol solutions. These were found to be 45 ps for τ_1, the intermediate decay associated with X, and 350 ps for τ_2, the shallow long-term decay. The fact that these constants also adequately describe the kinetics of recombination in other solvents will be considered later.

(c) Dynamics of Recombination, and Possible Identity of X. Having outlined a kinetic scheme that can reproduce the data, the identity of X and the dynamics of its generation and decay remain to be determined. It is useful to compare our current results with a closely analogous system, the photodissociation and geminate recombination of the I_2^- ion in similar solvents.[17−19] As stated briefly in the Introduction, Barbara and co-workers found that practically all the caging and recombination take place directly, whereas the residual diffusive portion of geminate recombination contributes mildly to restoration of the reactants, giving rise to a shallow tapering of the data after 10 ps, in analogy with delays beyond 150 ps in our results. The similarity extends also to the escape probabilities, which are highest in acetonitrile solutions and smallest in water for diiodide photolysis as well. Despite the overall similarities, the X component of geminate recombination is not evident in the diiodide photolysis data.

The disappearance of X is accompanied by a simultaneous reappearance of I_3^- and does not require mass diffusion to take place. Had that been the case, no match of time scales would be expected for both the intermediate phase of I_3^- bleach decay and that of diiodide absorption. Accordingly, the X component must be due to an intermediate that already contains the necessary components for reconstitution of triiodide in close proximity. This could be a complex of diiodide and iodine that is formed through solvent caging but does not directly cross back to the ground potential surface, either because of the electronic state of the nascent fragments or because of geometrical restrictions characteristic of atom−diatom potentials.

According to Scheme 2, a simple spectral decomposition can provide a transient spectrum of X alone. In terms of eq 1 this is $\mathbf{B}(\lambda)$ and is plotted in Figure 9, which includes the total absorption spectrum at a delay of 11 ps, along with the component due to the free diiodide which is subtracted to obtain $\mathbf{B}(\lambda)$. The resulting spectrum is broader and red-shifted with respect to the I_2^- absorbance. It would also appear to be somewhat higher in oscillator strength, although the spectral range is not sufficient in order to determine to what degree this is true.

Pending a definite identification of X, it is useful to outline possible triatomic complexes that might match the behavior observed. The ∼4 eV photon energy is enough to create iodine in the $J = {}^1/_2$ or ${}^3/_2$ states, and previous analysis has assumed

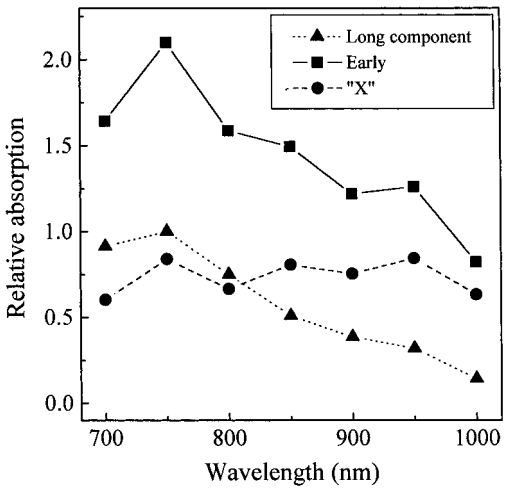

Figure 9. Coarse-grained spectrum of the X component in the range 700−1000 nm, from a spectral decomposition according to Scheme 2. See text for details.

production of that higher in energy. Assuming that both energetically allowed spin states are in fact generated, it is possible that relaxation of I* is required before recombination can take place with an adjacent diiodide ion. It is not trivial that recombination itself following electronic relaxation should be immediate, nor that such a spin flip should be activationless. Solvent relaxation would however have a limited effect upon its rate, possibly explaining the solvent independent decay times.

Other possibilities such as electronic relaxation of an excited diiodide ion or a stage of electron transfer (I_2^----I → I_2---I^-) might be invoked, but at least for the latter of these both a temperature and solvent dependence of the rate would be expected. As one may observe, the broad spectrum of X might also be suspected to stem from solvated electrons generated possibly through an ionization process which competes with photodissociation following 308 nm excitation. This can be ruled out since decay of solvated electrons would not be able to directly generate I_3^-. Furthermore, the differences in absorption spectrum and relaxation rates of solvated electrons in the various alcohols studied would be expected to give significant kinetic variations between data collected in ethanol and in isobutyl alcohol, which are not observed.[36] In both cases the onset of the biexponentially fit data commences after ∼10 ps in both the UV and IR probing, whereas the evolution of a free electron spectrum in these two solvents should be very different.

But regardless of the identity of X, the fact that this spectral component is present from the outset of recombination suggests a dynamical picture that is analogous with that outlined for I_2^- photolysis, whereby almost all solvent caging takes place during the initial stages of dissociation. Photoexcitation of the triiodide at 308 nm leads to a rapid stage of bond fission and caging which determines the ultimate destiny of the reactants. In this case, due to the structural complexity of the products, geminately caged fragments do not all recombine directly but bifurcate into two populations: those which cross over to the ground state directly and the X population that creates a long-lived intermediate within the cage, which requires longer delays to cross over to the reactant ground state. Thus, the two populations together are the counterparts in this process of the direct recombination component in diiodide photodissociation. Finally, the fact that the X absorption was not observed by Kuhne et al. may be due to the fact that there is a fundamental difference in the dynamics of triiodide dissociation when excitation is conducted at 390 nm and not 308 nm, especially in light of our speculation that this species might result from caging of electronically excited nascent fragments in states which might not be accessible to the less energetic reactants. To clear up these uncertainties, an ongoing Raman study of the evolving X/I_2^- is underway, as well as a study of reformation dynamics at various excitation photon energies and recombination of triiodide in highly viscous organic solvents.

(d) Solvent Effects. In view of the above scenario, it is worthwhile to consider the source of the strong solvent effects on this process. The effect of solvent on the vibrational relaxation of recombined triiodide and dephasing of the ground-state coherence which is observed during the fast portion of the regeneration of relaxed reactants has already been discussed. But one also observes that the solvent influences the overall escape probability and the relative amplitudes of the "fast" and X recombination components, as well as that of the residual slow taper.

Within the series of alcohols studied (methanol, ethanol, propanol, isobutyl alcohol) the escape probability decreases with an increase in size of the alcohol monomers. A similar effect has been reported for the capabilities of rare gas atoms to cage dissociating iodine molecules in clusters and fluid solutions.[5,13,17] One possible explanation for this is that the mass of the solvent molecule is instrumental in changing the momentum of separating fragments in solution—with the larger solvent being more effective at forcing a massive iodine fragment to crash back into its geminate partner. This however does not carry over to the case of water as solvent, possibly because of an increased effective mass for water due to its hypernetted character. The behavior in acetonitrile solutions, where the solvent molecule is also of smaller mass, does agree qualitatively with this trend.

Yet none of these considerations can explain the substantial differences in the partitioning of the recombinant population into the three components. Even though the escape probability is identical for water and isobutyl alcohol, the direct or "fast" component in water is more the 40% higher than in the larger alcohol. These differences must stem from solvent variations of the reaction dynamics during the act of bond fission and curve crossings at the early stages of photolysis. Until more precise potentials are available for this system it will be difficult to make sense of these numbers.

The solvent is known to effect other aspects of the reaction dynamics. In a Raman study of triiodide ions in polar solvents, Johnson et al. have demonstrated that the choice of solvent effects the degree of centrosymmetry of I_3^-, leading to almost perfect symmetry in acetonitrile and a fluctional displacement along the asymmetric stretch in ethanol solutions.[38] This breaking of symmetry is most likely the cause of the variation in the depth of the Raman excited spectral modulations observed in Figure 6, which are most pronounced in acetonitrile. The solvent-induced symmetry breaking was also demonstrated to effect the degree of compact coherence in the nascent I_2^- fragments following impulsive photolysis in this laboratory.[24] It is possible that this same mechanism is responsible for altering the relative contributions of the various recombination routes.

V. Conclusions

The caging and geminate recombination dynamics following the 308 nm photolysis of I_3^- in a series of polar solvents has been presented. The time resolution used has been ample to observe three temporal phases of reactant reformation, characterized by time scales of ∼2 ps, 45 ps, and one very long and

shallow component >350 ps in duration. The span of delay times studies has been shown to close the gap between femtosecond experiments and nanosecond studies of this reaction. The three components of geminate recombination are demonstrated to arise from independent kinetic pathways. The fate of photolysis fragments is interpreted to be determined shortly after the act of bond fission. According to a simple kinetic model used to analyze the data, caged fragments either recombine directly and vibrationally relax within a few picoseconds or produce long-lived complexes of unknown structure, which we have coined X in our discussion and which give rise to the ~40 ps component which decays exponentially. All three routes lead to ground-state I_3^-.

The persistent complex exhibits a near-IR absorption spectrum that is broadened and red-shifted relative to free I_2^-. The extremely shallow and slow residual component of recombination may be associated with encounters of geminate pairs that initially escape the solvent cage. Finally, choice of solvent strongly effects the probability and dynamics of caging, but not the rate of the decay of the complex caged pairs. This is not altered by varying the temperature of an isobutyl alcohol solution from 5 to 45 °C. The efficiency of caging in the various solvents suggests that the mass of solvent molecules may govern the probability of geminate recombination. Further experiments will be required for a definite identification of the X intermediate and to explain why it produces ground-state triiodide with a rate that is insensitive to both solvent viscosity and temperature. In any case, the existence of such an intermediate will need consideration in the continued 308 nm study of trihalide photochemistry on the ultrafast time scale.

Acknowledgment. We are indebted to Prof. Ronnie Kosloff, Prof. Noam Agmon, Mr. Guy Ashkenazi, Prof. P. F. Barbara, and Dr. P. K. Walhout for fruitful discussions and Prof. Anne B. Myers for sharing results prior to publication. We thank Dr. E. Mastov for technical assistance. This work was supported by the Israel Science Foundation. The Farkas Center is supported by the Bundesministerium fur die Forschung and the Minerva Gesellschaft fur die Forschung.

References and Notes

(1) Rabinovitch, E.; Wood, W. C. *Trans. Faraday Soc*. **1936**, *32*, 546.
(2) Noyes, R. M. *Prog. React. Kinet.* **1950**, *1*, 547.
(3) Otto, B.; Schroeder, J.; Troe, J. *J. Chem. Phys.* **1981**, *81*, 202.
(4) Bultmann, T.; Ernsting, N. P. *J. Phys. Chem.* **1996,** *100*, 19417.
(5) Lienau, C.; Zewail, A. H. *J. Phys. Chem.* **1996,** *100*, 18629.
(6) Scherer, N. F.; Ziegler, L. D.; Fleming, G. R. *J. Chem. Phys*. **1992**, *96*, 5544.
(7) Scherer, N. F.; Jonas, D. M.; Fleming, G. R. *J. Chem. Phys*. **1993**, *99*, 153.
(8) Ben Nun, M.; Levine, R. D.; Fleming, G. R. *J. Chem. Phys*. **1996**, *105*, 3035.
(9) Harris, A. L.; Brown, J. K.; Harris, C. B. *Annu. Rev. Chem. Phys.* **1988**, *39*, 341.
(10) Zadoyan, R.; Li, Z.; Ashjian, P.; Martens, C. C.; Apkarian, V. A. *Chem. Phys. Lett.* **1994**, *218*, 504.
(11) Zadoyan, R.; Sterling, M.; Apkarian, V. A. *J. Chem. Soc., Faraday Trans.* **1996**, *92*, 1821.
(12) Batista, V. S.; Coker, D. F. *J. Chem. Phys*. **1996**, *105*, 4033.
(13) Materny, A.; Lienau, C.; Zewail, A. H. *J. Phys. Chem.* **1996,** *100*, 18650.
(14) Papanikolas, J. M.; Vorsa, V.; Nadal, M. E.; Campagnola, P. J.; Lineberger, W. C. *J. Chem. Phys*. **1992**, *97*, 7002.
(15) Perera, L.; Amar, F. *J. Chem. Phys*. **1989**, *90*, 7354.
(16) Papanikolas, J. M.; Maslen, P. E.; Parson, *J. Chem. Phys*. **1995**, *102*, 2452.
(17) Alfano, J. C.; Kimura, Y.; Walhout, P. K.; Barbara, P. F. *Chem. Phys*. **1993**, *175*, 147.
(18) Walhout, P. K.; Alfano, J. C.; Thakur, K. A. M.; Barbara, P. F. *J. Phys. Chem.* **1995,** *99*, 7568.
(19) Benjamin, I.; Barbara, P. F.; Gertner, B. J.; Hynes, J. T. *J. Phys. Chem.* **1995,** *99*, 7557.
(20) Banin, U.; Waldman, A.; Ruhman, S. *J. Chem. Phys.* **1992**, *96*, 2416.
(21) Banin, U.; Ruhman, S. *J. Chem. Phys.* **1993**, *98,* 4391.
(22) Banin, U.; Kosloff, R.; Ruhman, S. *Isr. J. Chem.* **1993**, *33***,** 141.
(23) Banin, U.; Kosloff, R.; Ruhman, S. *Chem. Phys.* **1994**, *183***,** 289.
(24) Gershgoren, E.; Gordon, E.; Ruhman, S. *J. Chem. Phys.* **1997**, *106***,** 4806.
(25) Benjamin, I.; Banin U.; Ruhman, S. *J. Chem. Phys.* **1993**, *98*, 8337.
(26) Ashkenazi, G.; Kosloff, R.; Ruhman, S.; Tal-Ezer, H. *J. Chem. Phys.* **1995**, *103*, 5547.
(27) Ashkenazi, G.; Banin, U.; Bartana, A.; Kosloff, R.; Ruhman, S. *Adv. Chem. Phys.* **1997**, *100*, 229.
(28) Kuhne, T.; Vohringer, P. *J. Chem. Phys.* **1996**, *105*, 10788.
(29) Chesnoy, J.; Mokhtari, A. *Phys. Rev. A* **1988**, *38*, 3566.
(30) Banin, U.; Bartana, A.; Ruhman, S.; Kosloff, R. *J. Chem. Phys.* **1994**, *101*, 8461.
(31) Fournier De Violet, P.; Bonneau, R.; Joussot-Dubien, J. *Chem. Phys. Lett.* **1974**, *28*, 569.
(32) Kliner, D. A. V.; Alfano, J. C.; Barbara, P. F. *J. Chem. Phys.* **1993**, *98*, 5375.
(33) Baxendale, J. H.; Sharpe, P.; Ward, M. D. *Int. J. Radiat. Phys. Chem.* **1975**, *7*, 587.
(34) Kaya, K.; Mikami, M.; Udagawa, Y.; Ito, M. *Chem. Phys. Lett.* **1972**, *16*, 151.
(35) Gordon, E. M.Sc. Thesis, Jerusalem, 1997**.**
(36) Kenney-Wallace, G. A. *Adv. Chem. Phys.* **1981**, *47*, 535.
(37) Wan, C.; Gupta, M.; Baskin, J. S.; Kim, Z. H.; Zewail, A. H. *J. Chem. Phys.* **1997**, *106*, 4353.
(38) Johnson, A. E.; Myers, A. B. *J. Phys. Chem.* **1996**, *100*, 7778.